



PERGAMON

Acta mater. Vol. 47, No. 3, pp. 769–777, 1999
© 1999 Acta Metallurgica Inc.
Published by Elsevier Science Ltd. All rights reserved
Printed in Great Britain
1359-6454/99 \$19.00 + 0.00

PII: S1359-6454(98)00406-6

EXPERIMENTAL INVESTIGATION AND GINZBURG– LANDAU MODELING OF THE MICROSTRUCTURE DEPENDENCE OF SUPERCONDUCTIVITY IN Cu–Ag–Nb WIRES

D. RAABE† and D. MATTISEN

Institut für Metallkunde und Metallphysik, RWTH Aachen, 52056 Aachen, Germany

(Received 16 June 1998; accepted 23 November 1998)

Abstract—The type-II superconducting properties of heavily deformed Cu–Ag–Nb wires, containing only 4 wt% (4.18 vol.%) of elongated Nb filaments as a separate superconducting phase, were investigated as a function of microstructure, temperature, total wire strain, and external magnetic fields. The microstructure of the wires was examined using optical and electron microscopy. The experimental observation of the proximity effect, i.e. of the penetration of the superconducting state into the normal resistive Cu–Ag matrix leading to bulk-superconductivity, is explained in terms of the experimentally determined topology of the microstructure in conjunction with Ginzburg–Landau theory. The pronounced drop of the critical temperature and of the critical magnetic field with increasing wire strain is explained in terms of the reduced thickness of the ductile Nb filaments which is at large strains of the order of the Ginzburg–Landau correlation length in Nb. © 1999 Acta Metallurgica Inc. Published by Elsevier Science Ltd. All rights reserved.

1. INTRODUCTION

Ternary metal matrix composites consisting of Cu as matrix metal, a non-soluble body-centered cubic refractory metal such as Nb or Cr as a second phase, and face-centered cubic Ag as a precipitated second phase, Cu–Ag eutectic, or solid Cu–Ag solution, represent a recently introduced class of functional materials with high strength and high resistive conductivity [1–3] for applications in robotics and high field magnet design [4–8]. Since alloys consisting of Cu, Nb, and Ag are very ductile at room temperature, fiber reinforced metal matrix composite wires or foils can be produced by an *in situ* process, i.e. by melting, casting, swaging, and heavy wire drawing or cold rolling. The process can be complemented by an adequate heat treatment for optimizing the precipitation state of the Ag. Composites containing 8.2 wt% Ag and 4 wt% Nb (Cu balance) were observed to provide an optimal profile in terms of mechanical response, process technology, and electrical properties [1–3]. During the imposed large degrees of deformation both the Nb and the precipitated Ag gradually form into thin elongated filaments. After very large true (logarithmic) wire strains of up to $\eta = 10.5$ [$\eta = \ln(A_0/A)$ where A is the actual wire cross section and A_0 the initial wire cross section], filaments

with an average thickness of only a few nanometers can be observed.

Whilst the mechanical and resistive electromagnetic properties of heavily drawn Cu–8.2 wt% Ag–4 wt% Nb composite wires have been the subject of recent studies [1–3], their unusual superconducting properties have not yet been investigated. In this context two experimental observations attract particular attention, namely, first, the pronounced proximity effect and second, the strong influence of microstructure on the stability of the superconducting state in this material. The proximity effect, which phenomenologically describes the electronic influence that superconductors and normal resistive metals exert on each other across a common interface, manifests itself in the fact that a composite, which contains only 4 wt% (4 wt% Nb = 4.18 vol.% Nb) of the type-II superconducting Nb phase, shows a transition from the normal to the superconducting state at a critical temperature close to that of pure Nb [$T_c(\text{Nb}) = 9.2$ K]. The strong influence of the filament morphology and topology on the stability of the superconducting regime is evident from the observed drop of the critical temperature and of the critical magnetic field with increasing wire strain at constant sample current density.

In view of these observations, the objective of this paper is the investigation of the superconducting properties of heavily wire drawn Cu–8.2 wt% Ag–4 wt% Nb composite wires and the interpret-

†To whom all correspondence should be addressed.

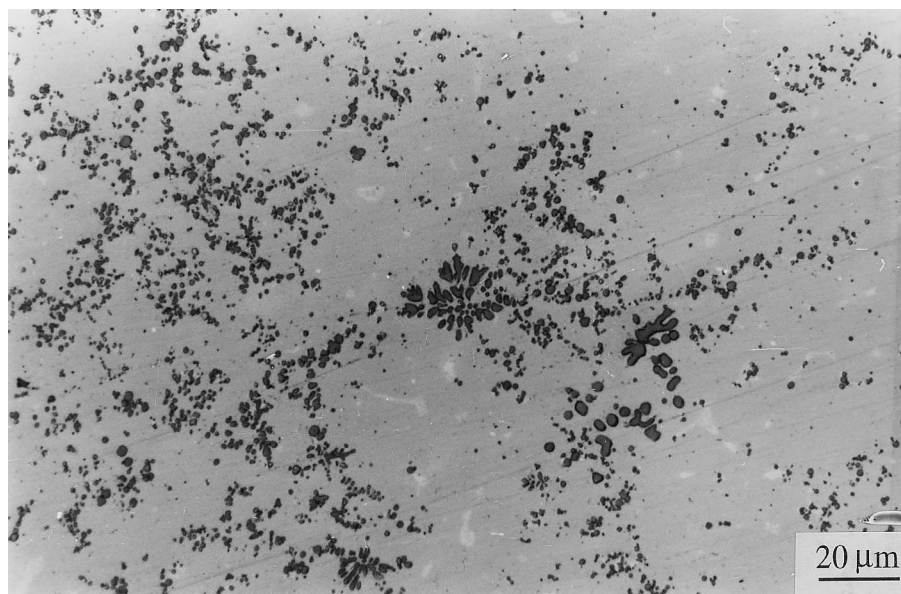


Fig. 1. Optical micrograph of the as-cast Cu–8.2 wt% Ag–4 wt% Nb sample. The dark areas are Nb. The white areas are Cu–Ag eutectic and Ag precipitations.

ation of these properties on the basis of microstructure and Ginzburg–Landau theory.

2. WIRE MANUFACTURING

A Cu–8.2 wt% Ag–4 wt% Nb alloy was prepared by inductive melting at a frequency of 10 kHz and a generator power of 50 kW using a crucible of high purity graphite. Due to the possibility of a miscibility gap in the liquid phase resulting from the presence of foreign interstitials, a peak temperature of 1830–1850°C was employed in order to assure complete dissolution of the Nb. Cylindrical ingots of 18 mm diameter were cast under Ar atmosphere at a pressure of 0.6×10^5 Pa into a preheated mould of high purity graphite. From the as-cast ingots cylindrical samples were prepared by grinding and rotary swaging. Wires were subsequently manufactured by drawing the cylindrical samples through hard metal drawing bench dies without intermediate annealing. The final minimum wire thickness amounted to 0.1 mm corresponding to a maximum true (logarithmic) wire strain of $\eta = 10.5$. Further processing details were reported in Refs [1, 9, 10].

3. EXPERIMENTAL METHODS

The morphology and topology of the Cu, Ag, and Nb in the Cu–8.2 wt% Ag–4 wt% Nb wires were determined using optical microscopy, scanning electron microscopy (SEM), and energy-disperse X-

ray spectrometry (EDX). The morphology of isolated Nb filaments was also investigated by use of an etching technique, where the Cu and Ag were dissolved by dilute nitric acid.

The resistivity of the wires was measured as a function of wire strain (in the range $\eta = 3.5$ –10.5), temperature (in the range 4.2–300 K), and external magnetic fields (in the range 0–1.2 T) by means of the direct current (d.c.) four-probe technique using a similar sample current density in each measurement. This means that each conductivity measurement was separately carried out on an individual portion of wire with a length of 12–15 cm which had a given strain, i.e. a constant cross section. The sample current was then chosen in accord with the actual wire cross section in a way to obtain the same sample current density for different measurements independent of the sample diameter. The data were taken continuously during cooling.

4. EXPERIMENTAL RESULTS

4.1. Microstructure

Figure 1 shows an optical micrograph of the as-cast Cu–8.2 wt% Ag–4 wt% Nb sample. The dark areas are Nb. The white areas are Cu–Ag eutectic and Ag precipitations. After removing the Cu-matrix and the Ag by etching, the Nb appears in the form of Wulff polyhedra [Fig. 2(a)] and dendrites [Fig. 2(b)]. Figure 3 shows some isolated Nb filaments (matrix removed by etching) at a true wire strain of $\eta = 10.5$. Figure 4 shows the average diameter of the Nb filaments as a function of wire strain† between $\eta = 3.5$ and 9.5. At large strains the average Nb diameters were around or below 100 nm, e.g. $d_{Nb} = 113$ nm at $\eta = 7$, $d_{Nb} = 96$ nm at

†A reliable measurement of the Nb diameters between $\eta = 9.5$ and 10.5 is only possible by use of transmission electron microscopy.

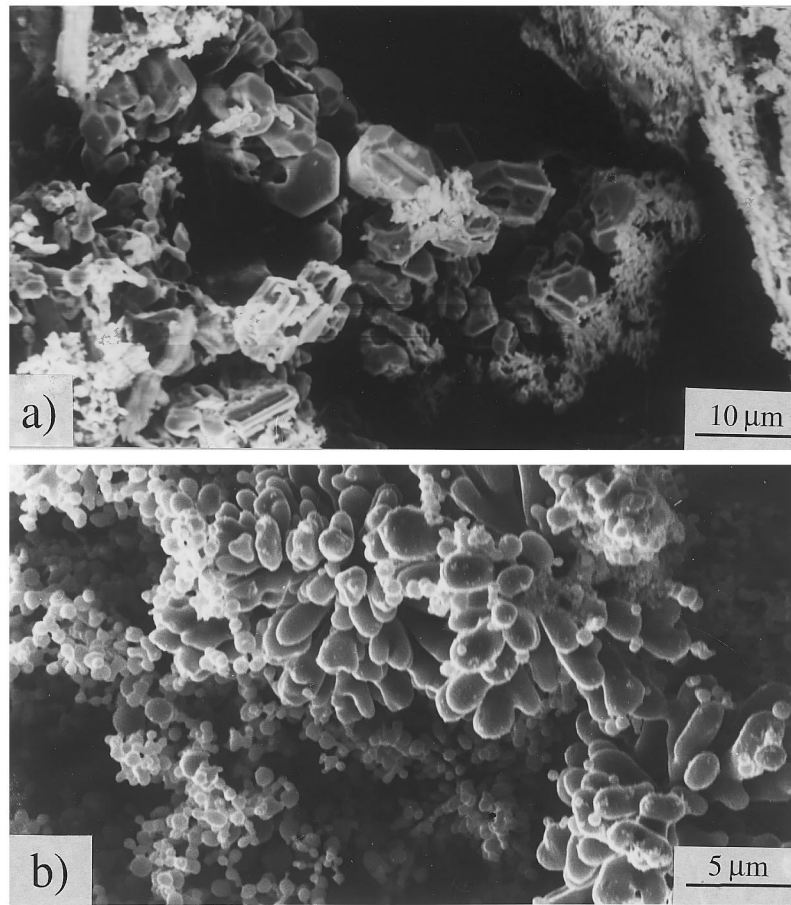


Fig. 2. After removing the Cu-matrix and the Ag by etching, the Nb appears in the form of Wulff polyhedra (a) and dendrites (b).

$\eta = 7.5$, $d_{\text{Nb}} = 86$ nm at $\eta = 8$, $d_{\text{Nb}} = 93$ nm at $\eta = 9.0$, and $d_{\text{Nb}} = 66$ nm at $\eta = 9.5$. The random arrangement of the dendrites in the micrograph (Fig. 3) is an artifact stemming from sample preparation. In the as-drawn composite, where the Nb is surrounded by Cu and Ag, the filaments are aligned parallel to the wire drawing axis.

4.2. Electromagnetic properties

Figure 5 shows the electrical resistivity of Cu–8.2 wt% Ag–4 wt% Nb as a function of temperature and wire strain. The inner figure magnifies the transition regime from the normal resistive to the superconducting state. The diagrams show that the normal state resistivity above the transition regime increases with the degree of wire strain. In the transition regime the critical temperature of the wires drops with increasing strain [Figs 5 and 6(a)], i.e. with decreasing average diameter of the Nb filaments [Fig. 6(b)]. The influence of strain and microstructure is even more pronounced for the decrease of the critical magnetic field with increasing wire strain [Fig. 6(c)] and decreasing average Nb diameter [Fig. 6(d)]. The critical values of transition are taken where the resistivity has fallen to 50% of the

normal conductive state. The range of transition was defined as the gap between the onset and offset values T_{onset} and T_{offset} or B_{onset} and B_{offset} , respectively (T = temperature in K, B = magnetic field in T). The various resistivity measurements were conducted with similar sample current densities, independent of the actual cross sections of the samples. Figure 7 shows the transition regime for the pure constituents Cu, Ag, and Nb.

5. APPLICATION OF GINZBURG–LANDAU THEORY TO THE PROXIMITY EFFECT

Changes in the normal state conductivity of a resistive metal due to the influence of an abutting superconductor and changes in the superconductivity of a superconductor due to the influence of an abutting resistive metal are referred to as proximity effects [11].

In the present case of Cu–8.2 wt% Ag–4 wt% Nb wires which show bulk superconductivity, the proximity effect can be used to explain the penetration of the superconducting state that exists in the Nb filaments into the normal resistive Cu–Ag matrix which by itself does not have intrinsic super-

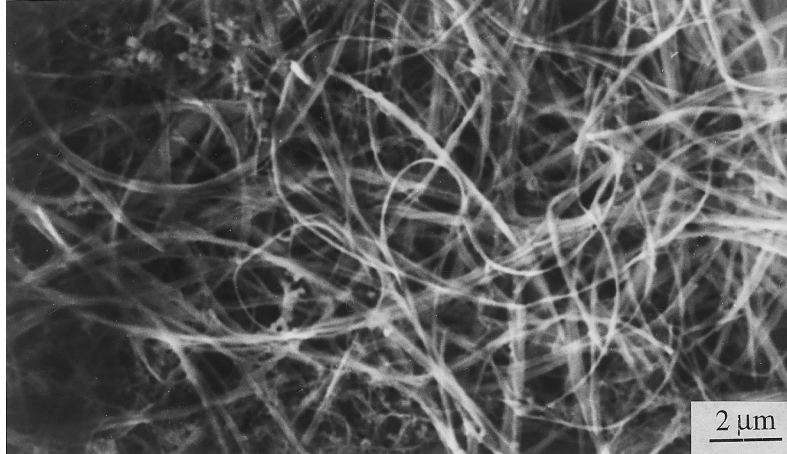


Fig. 3. Some isolated Nb filaments (matrix removed by etching) at a true wire strain of $\eta = 10.5$. The random arrangement of the dendrites stems from sample preparation. In the as-drawn composite, where the Nb is surrounded by Cu and Ag, the filaments are aligned parallel to the wire drawing axis.

conducting properties. In this context it is of particular importance to understand how a composite wire which contains only 4 wt% of the superconducting Nb phase (4 wt% Nb = 4.18 vol.% Nb) can reveal transition from the normal to the superconducting state altogether at a temperature close to the transition temperature of pure Nb [$T_c(\text{Nb}) = 9.2 \text{ K}$]. Since no Nb filaments were observed to have a length comparable to the distance between the voltage leads (12–15 cm) it is not possible that a continuous connection of Nb filaments existed over the distance examined. The observed bulk superconductivity of the wires can hence only be explained in terms of the occurrence of weak links between the Nb filaments, i.e. in terms of a local penetration of the superconducting state into the Cu–Ag matrix (proximity effect).

The proximity effect can be predicted using Ginzburg–Landau theory [12]. The order parameter in the Ginzburg–Landau equation Ψ has the meaning of the wave function of Cooper pairs present in the Bose condensate. In the absence of an external magnetic field in a bulk superconductor Ψ is independent of spatial coordinates. Near the critical temperature Ψ is small and the free energy density g may be expanded into a Landau-type† series in powers of $|\Psi|^2$

$$g(|\Psi|^2) = g_0 + a|\Psi|^2 + \frac{1}{2}b|\Psi|^4 + \dots \quad (1)$$

where a and b are coefficients which can be expanded in powers of $\tau = (T - T_c)/T_c$, where T_c is the critical temperature. Following a model by Abrikosov [13] one can now consider a superconductor (here: Nb) at a temperature slightly below its transition temperature $T_c(\text{Nb})$, which has an

†The introduction of a quadratic term as basis for the expansion is pertinent since the wave function is a complex quantity whilst the energy is a real quantity.

interface with a normal resistive metal that either does not become a superconductor at all (here: Cu–Ag matrix) or has a critical temperature far below $T_c(\text{Nb})$. Neglecting at first the filament morphology of the Nb we assume that the interface separates two semi-infinite one-dimensional bulk metals (Nb and Cu–Ag matrix). Abrikosov [13] showed that for this case the integral of the Ginzburg–Landau equation is

$$\xi^2 \left(\frac{d\Psi}{dx} \right)^2 + \Psi^2 - \frac{1}{2}\Psi^4 = \frac{1}{2} \quad (2)$$

where x is the spatial coordinate and ξ the correlation length, which is also referred to as the Ginzburg–Landau parameter [12] or Pippard coherence length [14]. The wave function Ψ is expressed in units of $\Psi_0 = (\alpha|\tau|/b)^{1/2}$ with $\alpha = a/\tau = (aT_c)/(T - T_c)$. The constant on the right-hand side of equation (2) is derived from the condition that in the bulk of the superconductor in

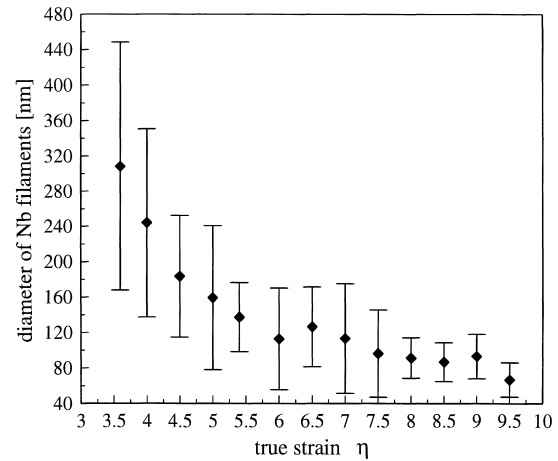


Fig. 4. Average diameter of the Nb filaments as a function of wire strain between $\eta = 3.5$ and 9.5.

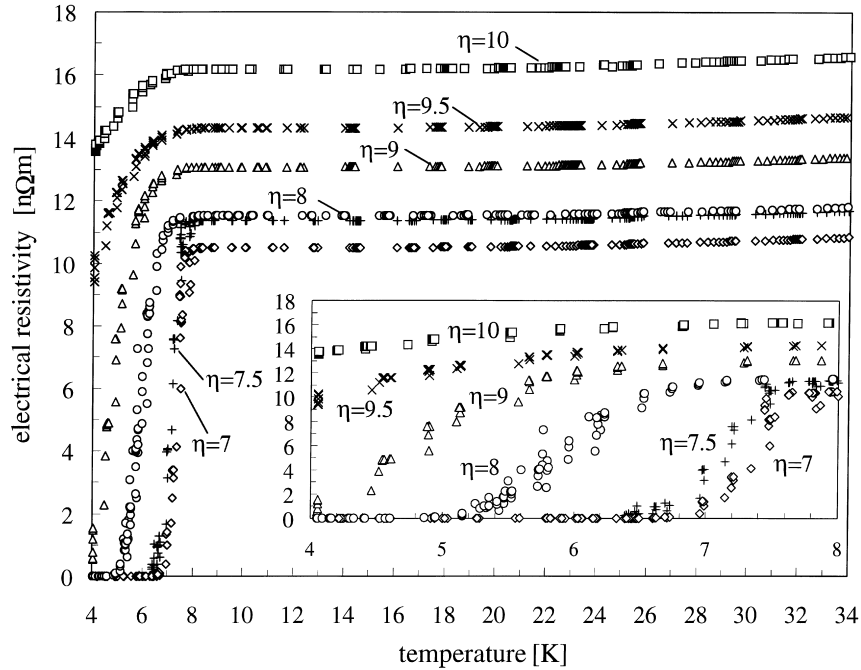


Fig. 5. Experimentally determined electrical resistivity of Cu–8.2 wt% Ag–4 wt% Nb wires as a function of temperature and wire strain (showing wire strains between 7 and 10). The inner figure magnifies the transition regime from the normal resistive to the superconducting state. The measurements were conducted with similar sample current densities.

the absence of an external magnetic field, $\Psi = 1$ and $(d\Psi/dx) = 0$. For a planar interface the boundary condition assumes the form

$$\left. \frac{d\Psi}{dx} \right|_{x=0} = \frac{1}{\tilde{\xi}} \Psi(0) \quad (3)$$

where $\tilde{\xi}$ is a correlation coefficient which can be determined in the framework of Bardeen–Cooper–Schrieffer theory [13, 15]. Zaitsev [16] showed that for pure superconductors $\tilde{\xi}$ amounts to $0.6 \cdot \xi_0$, where ξ_0 is the standard correlation length. ξ_0 can be calculated according to $\xi_0 = (0.18\hbar v_F)/(k_B T_c)$, where \hbar is Planck’s constant divided by 2π , v_F the Fermi velocity, and k_B Boltzmann’s constant. The solution of equation (2) assumes the form [13]

$$\Psi = \tanh\left(\frac{x - x_0}{\sqrt{2}\tilde{\xi}}\right). \quad (4)$$

The value of x_0 can be calculated from

$$\sinh\left(\frac{\sqrt{2}x_0}{\tilde{\xi}}\right) = -\frac{2\tilde{\xi}}{\xi}. \quad (5)$$

The temperature dependence of the Ginzburg–Landau parameter ξ is given by

$$\xi(T) = \frac{\xi_{T \rightarrow 0}}{\sqrt{1 - (T/T_c)}}. \quad (6)$$

For temperatures close to 0 K the literature suggests a value for the Ginzburg–Landau parameter of 39 nm [17–19]. Combining equations (4)–(6) then allows one to calculate the proximity effect at an

interface between the superconducting Nb phase and the resistive Cu–Ag matrix (Fig. 8).

6. DISCUSSION

6.1. Basic physical phenomena

In the interpretation of the experimental data one should distinguish between two physically different phenomena, the first one being the proximity effect which is held responsible for the existence of bulk superconductivity in an alloy with only 4.18 vol.% of the superconducting Nb phase (see Fig. 5) and the second one being the pronounced decrease of the critical temperature and of the critical magnetic field with increasing wire strain (see Fig. 6).

6.2. Proximity effect

Since there were no Nb filaments observed to have a length comparable to the distance between the voltage leads it is not likely that a closed superconducting percolation path solely along the Nb existed over the wire distance examined. The average diameter of the Nb particles in the as-cast state amounted to $d_{\text{Nb}} \approx 1481$ nm [2]. This means that in wires with a total strain of $\eta = 7$ the average length of the Nb filaments was $l_{\text{Nb}}(\eta = 7) = l_{\text{Nb}}^0 \cdot \exp(\eta) = 1.6$ mm. In contrast, the voltage leads had a spacing of 120–150 mm. This discrepancy is even more pronounced for less deformed wires which had an average filament length of only $l_{\text{Nb}}(\eta = 6) = 0.6$ mm and

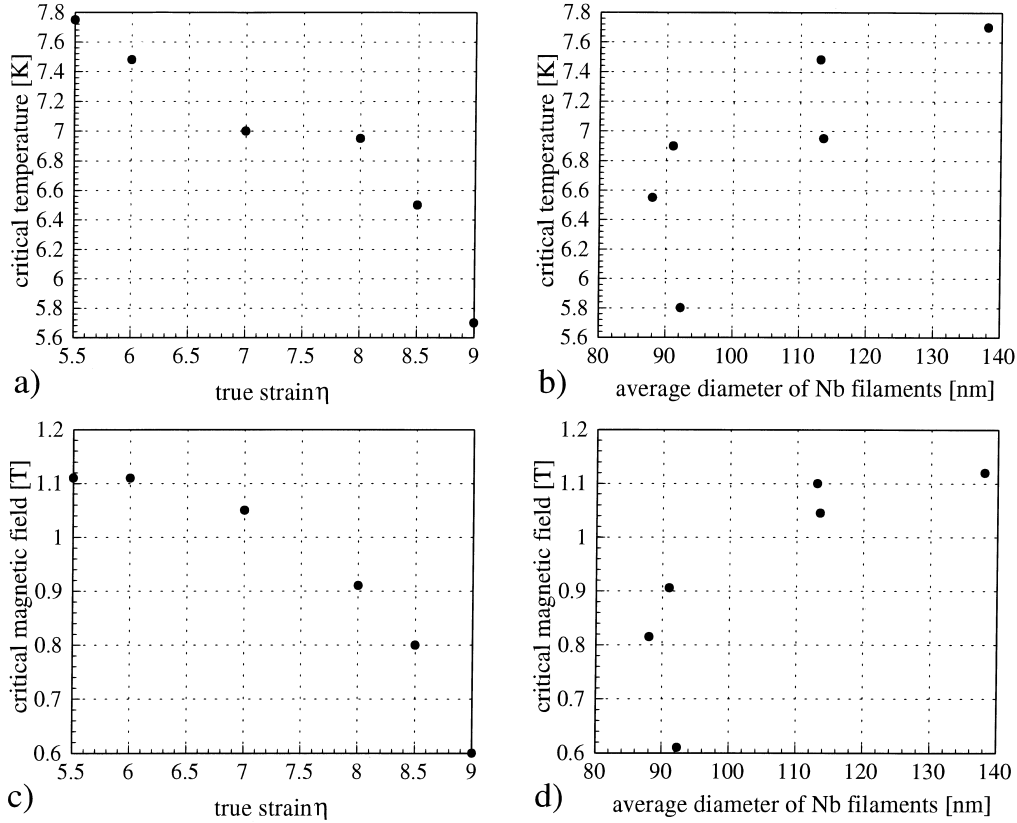


Fig. 6. Experimentally determined dependence of the critical temperature (a, b) and critical magnetic field (c, d) on wire strain and average diameter of the Nb filaments, respectively. The critical values of transition are taken where the resistivity has fallen to 50% of the normal conductive state. The range of transition was defined as the gap between the onset and offset values T_{onset} and T_{offset} or B_{onset} and B_{offset} , respectively (T = temperature in K, B = magnetic field in T). The measurements were conducted with similar sample current densities.

$l_{\text{Nb}}(\eta = 5.5) = 0.36$ mm. Nonetheless, samples of both wires showed a pronounced transition to the superconducting state (Fig. 9). The observed bulk-superconductivity of the Cu–8.2 wt% Ag–4 wt% Nb wires can thus only be attributed to the proximity effect, i.e. to the existence of weak links between the isolated Nb filaments where the superconducting state penetrates the Cu–Ag matrix (see Section 5).

The observation of weak links and their qualitative interpretation in terms of the proximity effect was already made in previous studies which investigated the resistivities of Cu based composites with about 15–20 vol.% Nb [20–24]. However, due to its low content of only 4.18 vol.% Nb, the explanation of bulk superconductivity is, in the case of the present alloy, less straightforward.

The analytical Ginzburg–Landau calculation (Fig. 8) shows that the predicted penetration range of the superconducting state into the Cu–Ag matrix is of the order of 100 nm. At first view this result of the calculation is not in good agreement with the microstructural data, which suggest a much larger average spacing between the neighboring parallel superconducting Nb filaments. The average spacing

between the Nb filaments $l_{\text{Nb}}^{\text{fit}}$ can be fitted from experimental data [1–3]. The data for the samples shown in Figs 5 and 9 are $l_{\text{Nb}}^{\text{fit}}(\eta = 5.5) = 3297$ nm, $l_{\text{Nb}}^{\text{fit}}(\eta = 6) = 2708$ nm, $l_{\text{Nb}}^{\text{fit}}(\eta = 7) = 2723$ nm, $l_{\text{Nb}}^{\text{fit}}(\eta = 7.5) = 2314$ nm, $l_{\text{Nb}}^{\text{fit}}(\eta = 8) = 2191$ nm, $l_{\text{Nb}}^{\text{fit}}(\eta = 9) = 2237$ nm, and $l_{\text{Nb}}^{\text{fit}}(\eta = 9.5) = 1602$ nm. The clear result that the fitted spacings exceed the proximity spacing, as predicted by Ginzburg–Landau theory, for all examined wires by more than one order of magnitude can be discussed in terms of five aspects.

First, it was shown by Verhoeven *et al.* [25, 26] that filament data determined by use of SEM are at large strains less accurate than those obtained by use of transmission electron microscopy. It must thus be taken into account, that the true average diameters of the Nb filaments might at large strains be smaller than those observed in the SEM and that their average spacings might consequently be lower than suggested by our fitted data. Second, it may be assumed that the Nb filaments are not exactly parallel so that their spacing might locally be much smaller than the fitted data suggest. Third, in cases where the current density is not too high, the existence of a closed superconducting percola-

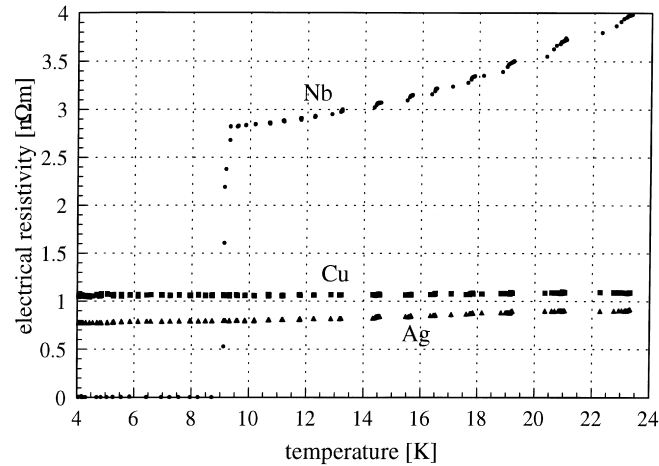


Fig. 7. Experimentally determined electrical resistivity in the transition regime for the pure constituents Cu, Ag, and Nb.

tion path along the Nb filaments is not only dependent on the *average* spacings but on the *minimum* occurring spacings between the Nb filaments. These minimum spacings can be much smaller than the average ones [2]. Fourth, it is conceivable that normal resistive Cu–Ag weak links existed between the Nb filaments, the residual resistive contributions of which were simply not detected due to the limited precision of the d.c. four-probe technique. Fifth, some limitations of the Ginzburg–Landau calcu-

lation might also explain the deviation, such as the exact value for the Pippard coherence length, the distance from the transition temperature of pure Nb, and the fact that the Nb has no semi-infinite extension.

6.3. Microstructure dependence of the critical temperature and of the critical magnetic field

The observed drop of the critical temperature and of the critical magnetic field with increasing

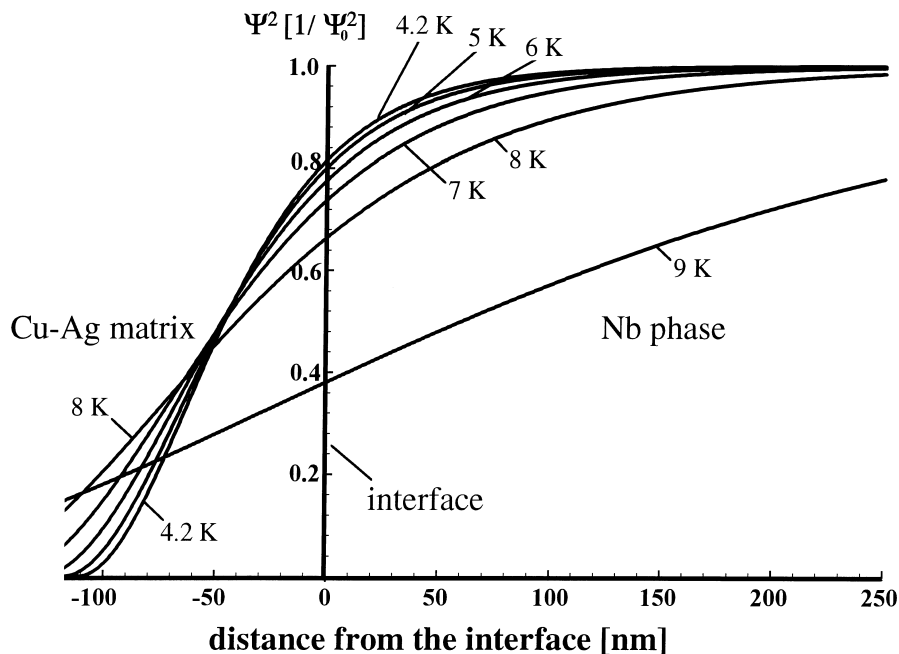


Fig. 8. Analytical Ginzburg–Landau calculation of the proximity effect at an interface between a one-dimensional superconducting Nb phase and a one-dimensional resistive Cu–Ag matrix. The plot shows the square of the order parameter in the Ginzburg–Landau equation Ψ , which has the meaning of the wave function of Cooper pairs present in the Bose condensate, in units of $\Psi_0 = (\alpha|\tau|/b)^{1/2}$ with $\alpha = a/\tau = (aT_c)/(T - T_c)$ where a and b are coefficients of the Landau-free-energy density form which can be expanded in powers of $\tau = (T - T_c)/T_c$. The result shows that the predicted penetration range of the superconducting state into the Cu–Ag matrix is of the order of 100 nm.

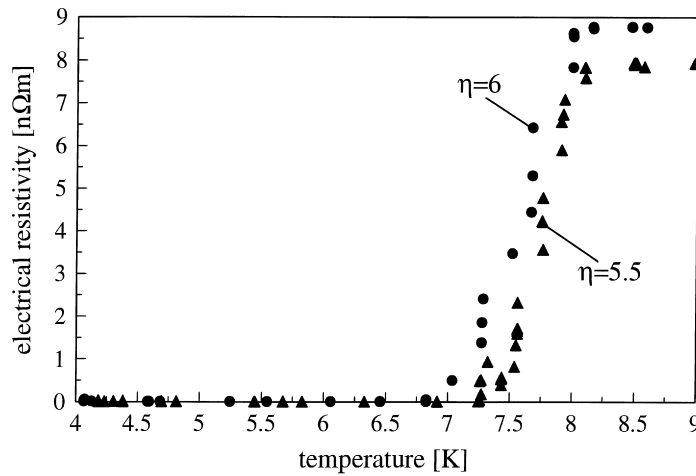


Fig. 9. Experimentally determined electrical resistivity of two Cu–8.2 wt% Ag–4 wt% Nb wires which had an average filament length of only $l_{\text{Nb}}(\eta = 6) = 0.6$ mm and $l_{\text{Nb}}(\eta = 5.5) = 0.36$ mm as a function of temperature and wire strain.

wire strain (see Fig. 6) cannot be explained on the basis of the calculation presented in Fig. 8. According to the proximity effect in the framework of Ginzburg–Landau theory, an increase of the filament length with increasing wire strain should lead to a better percolation and thus to a shift of the critical temperature towards that of pure Nb. However, this straightforward conclusion is in clear contradiction to our data which show exactly the opposite tendency (Figs 5, 6 and 9).

A likely explanation of this contradiction can be found in the microstructure of the Nb filaments. It is a well-known result of Ginzburg–Landau theory that thin type-II superconducting filaments, which have a thickness of the order of the correlation length, first change from type-II to type-I superconductors and gradually, with increasing strain, cease to be superconductive altogether [12, 13]. A similar effect was observed in a heavily rolled composite with about 20 vol.% Nb [21, 22]. For instance, at a temperature of 5.7 K, which is the transition temperature of wires with a total strain of $\eta = 9$ [Figs 5 and 6(a)], the correlation length of Nb amounts to 63 nm. This value is indeed very close to the average filament diameter of 93 nm. A similar observation holds for the other samples. This means that with increasing wire strain less and less Nb filaments can contain Cooper pairs due to their insufficient thickness. This gradual loss in the superconductivity of the Nb filaments entailing the loss of the bulk superconductivity as a function of their thickness distribution is well documented by the smeared out transition regime, particularly of the heavily deformed wires (see Fig. 5, small figure).

7. CONCLUSIONS

We investigated the superconducting properties of heavily drawn Cu–8.2 wt% Ag–4 wt% Nb com-

posite wires as a function of microstructure, temperature, total wire strain, and external magnetic fields. The main observations and results are:

- The observed proximity effect, i.e. the penetration of the superconducting state from the Nb filaments into the normal resistive Cu–Ag matrix, was explained in terms of the composite microstructure in conjunction with Ginzburg–Landau theory.
- The pronounced drop of the critical temperature and critical magnetic field with increasing wire strain was explained in terms of the reduced thickness of the ductile Nb filaments which is at large strains of the order of the Ginzburg–Landau correlation length in Nb.

Acknowledgements—The authors are indebted to L. P. Gor'kov, G. Gottstein, H.-J. Schneider-Muntau, and F. Heringhaus for valuable discussions. The kind support by the National High Magnetic Field Laboratory, Tallahassee, Florida, where the experiments were carried out has to be mentioned with gratitude (NHMFL grant with NSF DMR-9527035). One of the authors (D.R.) gratefully acknowledges the financial support by the Deutsche Forschungsgemeinschaft through the Heisenberg program and the kind support by the Department for Materials Science and Engineering at Carnegie Mellon University in Pittsburgh.

REFERENCES

1. Raabe, D. and Mattissen, D., *Metall*, 1997, **51**, 464.
2. Raabe, D. and Mattissen, D., *Acta Mater.* 1998, **46**, 5973–5984.
3. Raabe, D., Mattissen, D., Miyake, K., Takahara, H. and Heringhaus, F., in *Proceedings of the First International Conference "Composites at Lake Louise"*, Lake Louise, Alberta, Canada, Oct. 1997, ed. P. Nicholson, Eagle Press, Burlington, Ontario, Canada, 1997, p. 146.

4. Asano, T., Sakai, Y., Inoue, K., Oshikiri, M. and Maeda, H., *I.E.E.E. Magn.*, 1992, **28**, 888.
5. Heringhaus, F., Eyssa, Y. M., Pernambuco-Wise, P., Bird, M. D., Gottstein, G. and Schneider-Muntau, H.-J., *Metall*, 1996, **50**, 272.
6. Embury, J. D., Hill, M. A., Spitzig, W. A. and Sakai, Y., *MRS Bull.*, 1993, **8**, 57.
7. Heringhaus, F., Leffers, R., Gottstein, G. and Schneider-Muntau, H.-J., *Processing, Properties, and Application of Cast Metal Matrix Composites, TMS Fall Meeting*, Vol. 1, 1996, p. 127.
8. Schneider-Muntau, H.-J., *I.E.E.E. Trans. Magn.*, 1982, **18**, 32.
9. Heringhaus, F. and Raabe, D., *J. Mater. Proc. Technol.*, 1996, **59**, 367.
10. Mattissen, D., *Diplomarbeit*. Institut für Metallkunde und Metallphysik, RWTH Aachen, Germany, 1997 (in German).
11. Meissner, H., *Phys. Rev.*, 1958, **109**, 686 and 1958, **117**, 672.
12. Ginzburg, V. L. and Landau, L. D., *Zh. Éksp. Teor. Fiz.*, 1950, **20**, 1064.
13. Abrikosov, A. A., *Fundamentals of the Theory of Metals*. North-Holland, Amsterdam, 1988.
14. Pippard, A. B., *Proc. R. Soc. Lond. Ser.*, 1950, **A203**, 210.
15. Bardeen, J., Cooper, L. N. and Schrieffer, J. R., *Phys. Rev.*, 1957, **106**, 162 and 1957, **108**, 1175.
16. Zaitsev, R. O., *Zh. Éksp. Teor. Fiz.*, 1965, **48**, 664 and 1965, **48**, 1759.
17. Buckel, W., *Supraleitung*. VCH, Weinheim, 1990 (in German).
18. Parks, R. D., *Superconductivity*. Marcel Dekker, New York, 1969.
19. Saint-James, D., Sarma, G. and Thomas, E. J., *Type-II Superconductivity*. Pergamon Press, Braunschweig, 1969.
20. Raabe, D. and Heringhaus, F., *Physica status solidi (a)*, 1994, **142**, 473.
21. Raabe, D. and Hangen, U., *Acta metall.*, 1996, **44**, 953.
22. Raabe, D. and Hangen, U., *Physica status solidi (a)*, 1996, **154**, 715.
23. Foner, S. and Schwartz, B. B., *Superconductor Materials Science, Metallurgy, Fabrication, and Applications*, NATO Advanced Study Institute Series B: Physics. Plenum Press, New York, 1981.
24. Suenaga, M. and Clark, A. F., *Filamentary A15 Superconductors*. Plenum Press, New York, 1980.
25. Verhoeven, J. D., Spitzig, W. A., Schmidt, F. A., Krotz, P. D. and Gibson, E. D., *J. Mater. Sci.*, 1989, **24**, 1015.
26. Verhoeven, J. D., Chumbley, L. S., Laabs, F. C. and Spitzig, W. A., *Acta metall.*, 1991, **39**, 2825.